

# Facile Synthesis of Copper(II) Immobilized on Magnetic Mesoporous Silica Microspheres for Selective Enrichment of Peptides for Mass Spectrometry Analysis\*\*

Shasha Liu, Hemei Chen, Xiaohui Lu, Chunhui Deng,\* Xiangmin Zhang, and Pengyuan Yang

Magnetic nanoparticles have been applied in magnetic resonance imaging (MRI),<sup>[1]</sup> cell research,<sup>[2]</sup> and magnetically assisted drug delivery<sup>[3]</sup> because of their high liquid dispersibility, the ease of surface modification, and unique magnetic responsivity. Magnetite ( $\text{Fe}_3\text{O}_4$ ) is considered an ideal candidate for magnetic applications in biological and biomedical fields<sup>[4,5]</sup> because of its good hydrophilicity, biocompatibility, nontoxicity, and chemical stability. More recently, magnetite nanoparticles have emerged as a promising separation nanotool in proteome research.<sup>[6,7]</sup> In a peptidome study, endogenous peptides were recently shown to contain potential biomarkers for recording the physiological and pathological states of human beings. Much investigation has been directed toward the qualitative and quantitative study of endogenous peptides in complex biological samples,<sup>[8]</sup> because these biomarkers can potentially achieve more clinical sensitivity and specificity compared with common biomarkers.<sup>[9]</sup>

Many methodologies are currently used to enrich peptides from biological samples. Centrifugal ultrafiltration with accurate molecular weight (MW) cutoff is the most widely used method to extract peptides and remove proteins with higher MWs based on a size-exclusion mechanism;<sup>[10]</sup> however, the low efficiency of this method limits its practical application. The hydrophobic-based capture technique can remove salts and other hydrophilic compounds in a single step before MS analysis. For this technique, nanomaterials with high specific surface areas, for example, multiwalled carbon nanotubes, are preferred.<sup>[11]</sup> However, the bulk of protein mass can bind tightly on reversed phase (RP) absorbents at the expense of small peptide binding sites. Recently, MCM-41 particles, a typical ordered mesoporous silica materials, were found to show excellent performance in serum peptidome

enrichment<sup>[12]</sup> owing to their high surface area and uniform mesopores (2.0 nm), which allow the entrance of low-MW peptides but exclude large proteins based on size-exclusion mechanism. In our previous work,<sup>[13]</sup> magnetic mesoporous microspheres with hydrophobic surface were developed to enrich endogenous peptides in rat brain extraction; however, they can only capture specific hydrophobic peptides by the weak hydrophobic interaction between hydrophobic peptides and siloxane bridge groups on the pore wall inside mesopores. As is well known, many endogenous peptides are hydrophilic in biological samples; therefore, the hydrophilic peptides would be lost by using these kinds of reversed phase particles.

Immobilized metal ion affinity chromatography (IMAC) has allowed new applications in protein purification.<sup>[14–16]</sup> The IMAC technique for proteins and peptides is based on the reversible association–dissociation of the immobilized metal ions and target protein/peptide molecules. Specifically,  $\text{Cu}^{2+}$  ions can be immobilized on substrates and interact with amino acids chains of the peptides/proteins through coordination bond, and after enrichment the protein/peptide can be released through the disruption of coordination bond using eluting reagent. In view of the properties of magnetic materials and ordered mesoporous materials, and the advantages of the IMAC technique, the design and synthesis of nanomaterials combining the merits of metal ion affinity, size-exclusion, and magnetic separability for peptidome would be very important and interesting in proteomics.

Herein, we report a facile approach to synthesize  $\text{Cu}^{2+}$ -modified magnetic mesoporous silica microspheres (designated as  $\text{Fe}_3\text{O}_4@\text{mSiO}_2\text{-Cu}^{2+}$ ) with magnetite core and mesoporous silica shell for peptide enrichment. The mesoporous silica shells with perpendicularly aligned channels are formed directly on  $\text{Fe}_3\text{O}_4$  cores by a surfactant templating strategy, and the interior surface of the mesopores was modified with  $\text{Cu}^{2+}$  ions. The obtained microspheres possess high magnetization saturation ( $43.6 \text{ emu g}^{-1}$ ), uniform mesopore size (3.3 nm), high surface area ( $85 \text{ m}^2 \text{ g}^{-1}$ ), and abundant  $\text{Cu}^{2+}$  ions inside mesopores. By taking advantage of the highly open mesopore channels with numerous immobilized  $\text{Cu}^{2+}$  ions, we successfully applied the  $\text{Fe}_3\text{O}_4@\text{mSiO}_2\text{-Cu}^{2+}$  microspheres to capture peptides selectively and efficiently in complex biosamples.

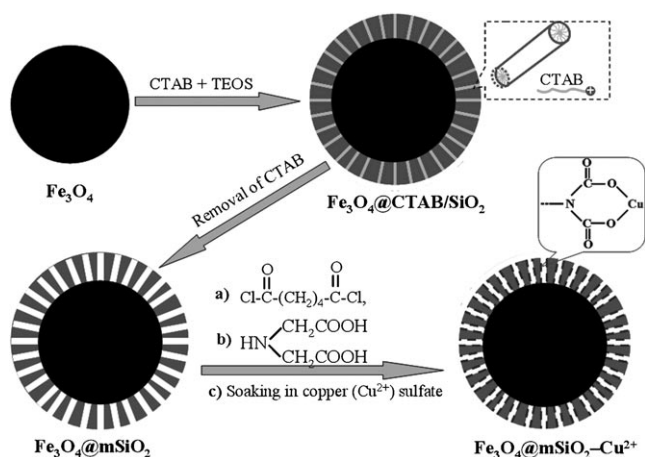
The main feature of  $\text{Fe}_3\text{O}_4@\text{mSiO}_2\text{-Cu}^{2+}$  microspheres is the facile one-step synthetic approach of directly coating mesoporous  $\text{SiO}_2$  shell on the magnetic  $\text{Fe}_3\text{O}_4$  particles (Scheme 1).  $\text{Fe}_3\text{O}_4$  particles were directly coated by a layer of mesostructured cetyltrimethylammonium bromide (CTAB)/silica composites through a sol–gel process by using

[\*] S. Liu, H. Chen, Prof. C. Deng, Prof. X. Zhang, Prof. P. Yang  
Department of Chemistry & Institutes of Biomedical Sciences  
Fudan University, Shanghai 200433 (China)  
Fax: (+86) 21-6564-1740  
E-mail: chdeng@fudan.edu.cn

X. Lu  
Center of Analysis and Measurement, Fudan University  
Shanghai 200433 (China)

[\*\*] The work was supported by the National Natural Science Foundation of China (20875017, 20735005), the Technological Innovation Program of Shanghai (09JC1401100), the National Basic Research Priorities Program (2007CB914100/3), and Shanghai Leading Academic Discipline Project (B109).

Supporting information for this article (including experimental details) is available on the WWW under <http://dx.doi.org/10.1002/anie.201003602>.



**Scheme 1.** Synthesis route to  $\text{Cu}^{2+}$ -modified magnetic mesoporous silica ( $\text{Fe}_3\text{O}_4@m\text{SiO}_2\text{-Cu}^{2+}$ ) core-shell microspheres.

CTAB as a structure-directing agent, and CTAB molecules were then removed by solvent extraction to form  $\text{Fe}_3\text{O}_4@m\text{SiO}_2$  microspheres that possess a magnetic core and an ordered mesoporous silica shell with open pore channels.<sup>[17]</sup> In the next step,  $\text{Cu}^{2+}$  ions were immobilized on the pore walls by surface grafting a carboxy-containing spacer and subsequent chelation of  $\text{Cu}^{2+}$  ions. The resulting  $\text{Fe}_3\text{O}_4@m\text{SiO}_2\text{-Cu}^{2+}$  microspheres were applied to the fast and effective enrichment of hydrophobic/hydrophilic peptides and simultaneously excluding high-MW proteins by virtue of the proper pore size and the affinity interaction of immobilized  $\text{Cu}^{2+}$  ions with carboxylic groups and amino groups of peptides (Scheme 2; experimental details are given in the Supporting Information).

Scanning electron microscopy (SEM) observation indicates that the  $\text{Fe}_3\text{O}_4@m\text{SiO}_2$  microspheres have regular spherical shape with an average diameter of 350 nm (Figure 1 a). The transmission electron microscopy (TEM) image reveals a core-shell structure of the microspheres, in which a dark core of magnetite (diameter: 250 nm) and a gray porous

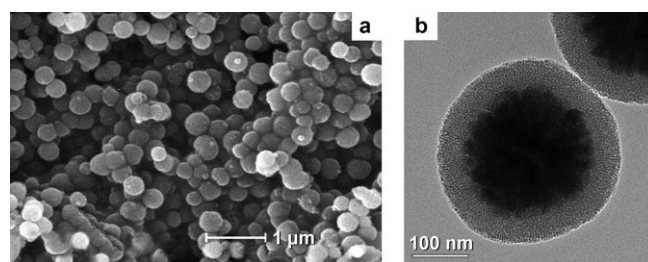
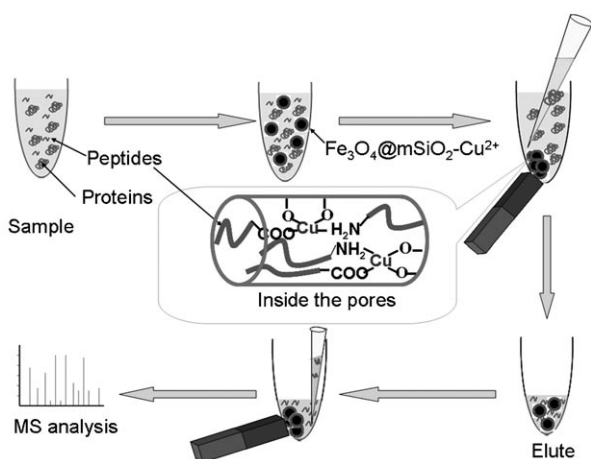


**Figure 1.** a) Representative scanning electron microscopy image and b) transmission electron microscopy image of the synthesized  $\text{Fe}_3\text{O}_4@m\text{SiO}_2$  microspheres.

silica shell (thickness: 50 nm) can be clearly seen owing to the dramatic mass contrast under TEM (Figure 1 b). Notably, the pore channels are perpendicularly aligned in the shell, which results from the unique co-assembly of CTAB/silica on the surfaces of the  $\text{Fe}_3\text{O}_4$  particles.<sup>[18]</sup> This preferred pore orientation significantly increases the surface area and provides accessibility for guest molecules. To immobilize  $\text{Cu}^{2+}$  ions, the  $\text{Fe}_3\text{O}_4@m\text{SiO}_2$  microspheres were activated by reaction first with hexanedioyl chloride (HC) and then with iminodiacetic acid (IA), and finally  $\text{Cu}^{2+}$  ions were introduced by soaking the HC-IA activated microspheres with copper sulfate solution (0.2 M). The obtained microspheres were further analyzed by TEM and SEM (Figure S1 in the Supporting Information), which indicate that the core-shell structure and ordered mesoporous shell with perpendicularly aligned pore channels were well retained in the microspheres (Figure S1a,b). The chemical composition of the obtained microspheres was examined by SEM-energy-dispersive X-ray spectroscopy (SEM-EDS) analysis (Figure S1c,d), and the copper content in the composites was measured to be 3.95% in mean atomic value, indicating an efficient chelation of  $\text{Cu}^{2+}$  ions owing to the high surface area of the mesoporous silica shell. Fourier transform infrared (FTIR) spectroscopy was employed to characterize both the  $\text{Fe}_3\text{O}_4@m\text{SiO}_2$  and  $\text{Fe}_3\text{O}_4@m\text{SiO}_2\text{-Cu}^{2+}$  microspheres (Figure S2a,b), in which typical absorption bands at  $581\text{ cm}^{-1}$  and  $1085\text{ cm}^{-1}$  are ascribed to Fe-O-Fe and Si-O-Si vibrations, respectively. Relative to  $\text{Fe}_3\text{O}_4@m\text{SiO}_2$  microspheres,  $\text{Fe}_3\text{O}_4@m\text{SiO}_2\text{-Cu}^{2+}$  microspheres display stronger bands at  $1401$  and  $1629\text{ cm}^{-1}$ , which can be assigned to the asymmetric C-O stretching and the symmetric C-O stretching vibrations of carboxylates formed after surface modification. These results further confirm the immobilization of  $\text{Cu}^{2+}$  ions on the  $\text{Fe}_3\text{O}_4@m\text{SiO}_2$  microspheres.

Wide-angle X-ray diffraction patterns exhibit well-resolved diffraction peaks for the obtained  $\text{Fe}_3\text{O}_4@m\text{SiO}_2\text{-Cu}^{2+}$  microspheres (Figure S3). All the peaks can be exactly indexed to the diffractions of magnetite phase, suggesting that the sol-gel process and surface modification have no effect on the crystalline properties of magnetite. The magnetic properties (Figure S4) of the  $\text{Fe}_3\text{O}_4@m\text{SiO}_2\text{-Cu}^{2+}$  microspheres were characterized with a superconductive quantum interference device (SQUID) at  $25^\circ\text{C}$ . The microspheres exhibit superparamagnetism; that is, no remanence was recorded when the applied magnetic field was removed, and the magnetization



**Scheme 2.** Workflow of fast and efficient approach of selective peptide enrichment protocol using  $\text{Fe}_3\text{O}_4@m\text{SiO}_2\text{-Cu}^{2+}$  core-shell microspheres and MALDI-TOF MS analysis.

saturation was calculated to be as high as  $43.6 \text{ emu g}^{-1}$ . The high magnetization endows the microspheres with fast responsiveness to applied magnetic field in magnetic separation.

The mesostructure of the  $\text{Fe}_3\text{O}_4@\text{mSiO}_2\text{-Cu}^{2+}$  microspheres was investigated by using low-angle X-ray diffraction (Figure 2a). The well-resolved diffraction peak at around  $2.3^\circ$  corresponds to the 100 reflection of a two-dimensional

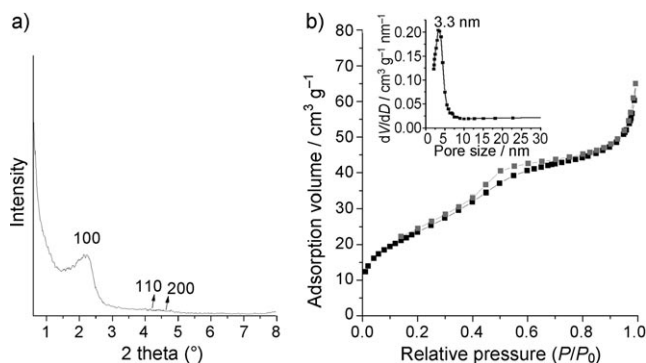


**Figure 2.** a) Low-angle X-ray diffraction pattern and b) nitrogen adsorption-desorption isotherms and pore size distribution (inset) of the  $\text{Fe}_3\text{O}_4@\text{mSiO}_2\text{-Cu}^{2+}$  microspheres.

hexagonal ordered mesostructure, and the other two peaks at round  $4.5^\circ$  are not so resolved owing to the short-range ordering features of the mesopore alignment on the spherical surface. Nitrogen sorption was performed to study the pore properties of the  $\text{Fe}_3\text{O}_4@\text{mSiO}_2\text{-Cu}^{2+}$  microspheres. As displayed in Figure 2b, the nitrogen adsorption-desorption isotherms of the microspheres exhibit a type-IV curve with small hysteresis, which indicates some interstitial structures form among the aggregated particles in the sample. The narrow pore size distribution derived from the adsorption branch using the Barrett-Joyner-Halenda (BJH) method indicates a mean pore size of 3.3 nm for the microspheres. The BET surface area and total pore volume were calculated to be  $85 \text{ m}^2 \text{ g}^{-1}$  and  $0.1 \text{ cm}^3 \text{ g}^{-1}$ , respectively, indicating a high degree of porosity.

The high surface area and large amount of immobilized  $\text{Cu}^{2+}$  ions enable the  $\text{Fe}_3\text{O}_4@\text{mSiO}_2\text{-Cu}^{2+}$  microspheres to efficiently enrich both hydrophilic and hydrophobic peptides by chelating with carboxylic and amino groups of peptides. Hydrophobic angiotensin II (linear peptides, sequence: DRVYIHPF) and hydrophilic microcystin-LR (MC-LR, cyclic peptide; see Figure S5) were used as model samples to attain enrichment efficiency of our functional microspheres.<sup>[6b,c,e]</sup> The workflow of the peptides enrichment is illustrated in Scheme 2.

As revealed by the mass spectra analysis, an aqueous solution of angiotensin II at a concentration of 5 nM, which is difficult to detect, shows signal-to-noise (S/N) ratio of only 25.18 (Figure 3a). However, after enrichment (Figure 3b) with the  $\text{Fe}_3\text{O}_4@\text{mSiO}_2\text{-Cu}^{2+}$  microspheres, the S/N ratio increases to 1017.33, indicating an enrichment factor (EF) of about 40. Similarly, for MC-LR solution, the S/N ratio of the solution at a concentration of 5 nM increases from 27.05 to 951.62 after enrichment for 2 min, indicating an EF of about

35 (Figure 3c,d). These results demonstrate the excellent performance of  $\text{Fe}_3\text{O}_4@\text{mSiO}_2\text{-Cu}^{2+}$  microspheres in enriching both hydrophobic and hydrophilic peptides. To demonstrate further the effect of immobilized  $\text{Cu}^{2+}$  ions on the enrichment efficiency, control experiments were conducted by using  $\text{Fe}_3\text{O}_4@\text{mSiO}_2$  microspheres before and after surface modification as the absorbents for angiotensin II (Figure S6). As displayed in Figure S6f (see the Supporting Information), the  $\text{Fe}_3\text{O}_4@\text{mSiO}_2$  microspheres without modification show an EF of 4.1, mainly contributed by the high surface area, and the HC-IA modified  $\text{Fe}_3\text{O}_4@\text{mSiO}_2$  microspheres exhibit an EF of 6.9, which is slightly larger than that of  $\text{Fe}_3\text{O}_4@\text{mSiO}_2$  microspheres, indicating limitation of the HC-IA organic

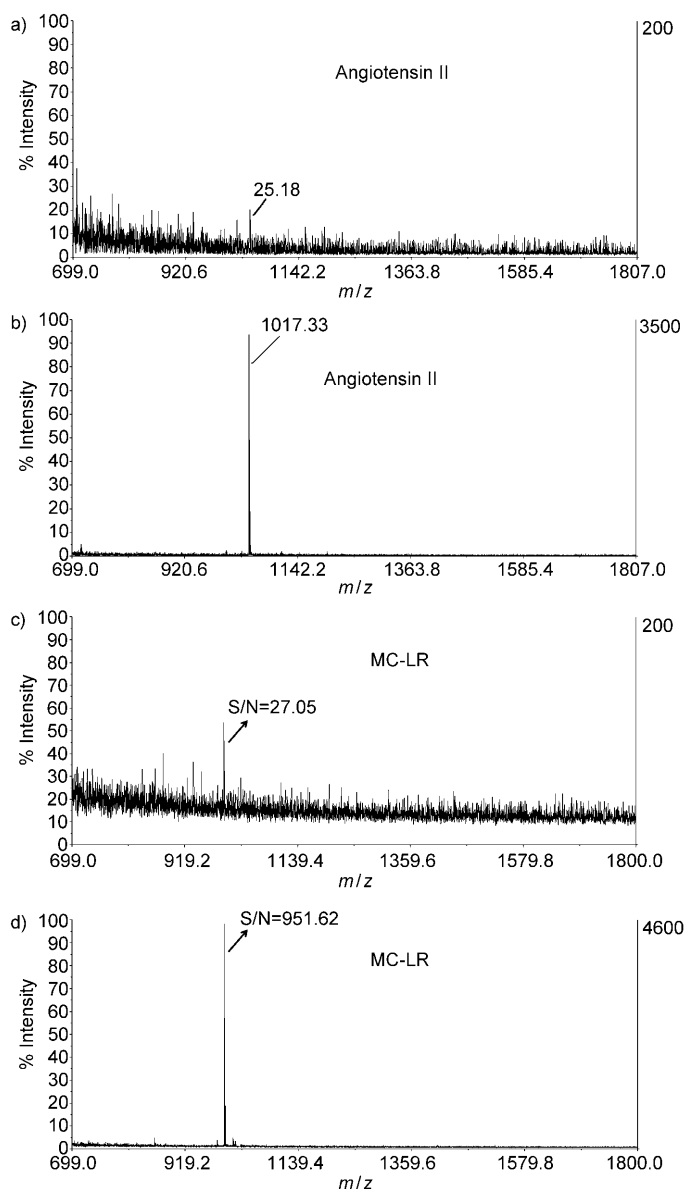


**Figure 3.** MALDI-TOF mass spectra of a) 5 nM angiotensin II (MW = 1046.2, isoelectric point (pI) = 6.74) without any treatment, b) 5 nM angiotensin II after enrichment by  $\text{Fe}_3\text{O}_4@\text{mSiO}_2\text{-Cu}^{2+}$  microspheres, c) 5 nM MC-LR (MW = 995.5) without any treatment, d) 5 nM MC-LR (MW = 995.5) after enrichment by  $\text{Fe}_3\text{O}_4@\text{mSiO}_2\text{-Cu}^{2+}$  microspheres.

moieties in peptide enrichment. Notably, after soaking in a low-concentration  $\text{CuSO}_4$  solution (0.02 M), the resultant  $\text{Fe}_3\text{O}_4@\text{mSiO}_2\text{-Cu}^{2+}$  microspheres show a significantly large EF of 16.0, suggesting that the  $\text{Cu}^{2+}$  ions immobilized inside mesopores can capture peptides efficiently. Soaking the microspheres in higher concentration  $\text{CuSO}_4$  solution (0.1 M and 0.2 M, respectively) can further increase the  $\text{Cu}^{2+}$  contents in microspheres (see Figure S7 and Figure S1, respectively) and achieve EF values of 31.3 and 40.4, respectively. These results reveal a direct relationship between the immobilized  $\text{Cu}^{2+}$  content and their enrichment capacity and thus demonstrate a high efficiency of the novel functionalized magnetic mesoporous microspheres in peptide enrichment.

In addition, tryptic bovine serum albumin (BSA) digest was applied to investigate the efficiency of the functional microspheres. From Figure S8 and Table S1 (see the Supporting Information), it can be seen that the  $\text{Fe}_3\text{O}_4@\text{mSiO}_2\text{-Cu}^{2+}$  microspheres could enrich hydrophilic/hydrophobic peptides ranging from grand average of hydropathy (GRAVY) =  $-1.723$  to  $0.292$  without discrimination. These results provide additional evidence that the  $\text{Fe}_3\text{O}_4@\text{mSiO}_2\text{-Cu}^{2+}$  microspheres can serve as a versatile absorbent in enrichment of universal peptides. Biosamples often contain a mass of proteins, which makes it difficult to identify peptides from the original biosamples, such as serum, urine, and tissue extracts. The complexity of biosamples also affects the current peptidome techniques, because the coexisting high-abundant proteins can also be absorbed on the absorbent surface. Since the obtained microspheres provide an excellent size-exclusion effect,<sup>[13,14]</sup> magnetic separability, and specific affinity, it is feasible to enrich peptides selectively from biosamples through the size-exclusion effect.

Human serum contains a complex array of proteolytically derived peptides (serum peptidome), which might be biomarkers of preclinical screening and disease diagnosis. To investigate the size-exclusion effect, the microspheres were further applied to enrichment of peptides from human serum according to the previous protocol.<sup>[6c]</sup> A suspension of  $\text{Fe}_3\text{O}_4@\text{mSiO}_2\text{-Cu}^{2+}$  microspheres (20  $\mu\text{L}$ , 10  $\text{mg mL}^{-1}$ ) was added to a solution of diluted serum (500  $\mu\text{L}$ , containing 100  $\mu\text{L}$  of pristine serum), which was vibrated for 10 min. The microspheres with peptides were collected and treated using the strategy described previously. Figure 4 shows the mass spectra of peptides profiling before and after enrichment by  $\text{Fe}_3\text{O}_4@\text{mSiO}_2\text{-Cu}^{2+}$  microspheres from human serum. It indicates that numerous peptides were successfully enriched and separated at a mass range from 800 to 3500 Da, although no peptide could be identified in diluted serum samples at a low concentration. In addition, human urine was applied to evaluate the selective enrichment ability. An effective enrichment of urine peptides at a low MW from 800 to 3500 Da is also accomplished (Figure S9). These results suggest that the  $\text{Fe}_3\text{O}_4@\text{mSiO}_2\text{-Cu}^{2+}$  microspheres have high potential in peptide enrichment from complex biosamples.

In conclusion,  $\text{Cu}^{2+}$ -modified core-shell magnetic mesoporous silica microspheres were facily synthesized through a surfactant-templated sol-gel process and subsequent chelation of  $\text{Cu}^{2+}$  ions. The obtained microspheres possess high magnetization saturation (43.6  $\text{emu g}^{-1}$ ), large surface area

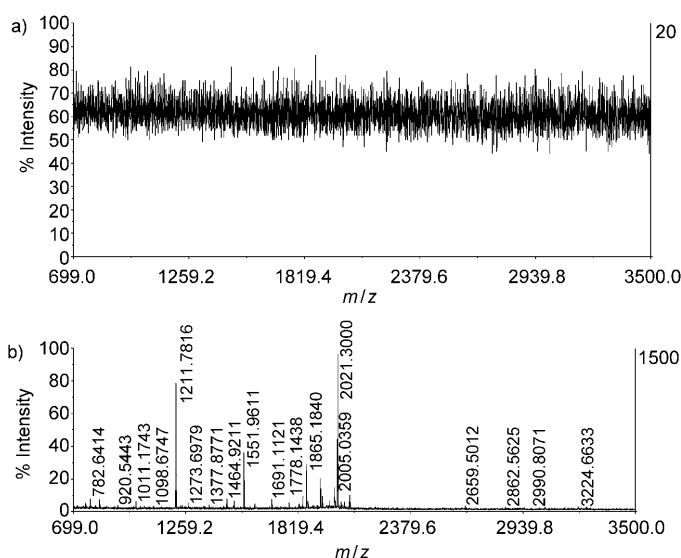


**Figure 4.** The MALDI-TOF mass spectra of human serum solution a) without any treatment; b) enriched by  $\text{Fe}_3\text{O}_4@\text{mSiO}_2\text{-Cu}^{2+}$  microspheres and eluted with 0.4 M amino solution.

(85  $\text{m}^2 \text{g}^{-1}$ ), accessible uniform mesopores of 3.3 nm, as well as high-density immobilized  $\text{Cu}^{2+}$  ions. The microspheres were then successfully applied to enrich hydrophobic and hydrophilic peptides from standard peptides solution and tryptic protein digest solution. More importantly, it was demonstrated that the functional microspheres can capture peptides selectively from complex sample systems (such as human serum and urine) with the large proteins excluded. Because the microspheres combine the merits of the magnetic property of  $\text{Fe}_3\text{O}_4$ , the porosity of mesoporous silica, and the specific affinity of  $\text{Cu}^{2+}$  ions toward peptides, the process of selective peptides enrichment is very convenient and efficient. Consequently, this technique is expected to open up new horizons for the enrichment of endogenous peptides, as well as new applications of magnetic mesoporous materials.

Received: June 13, 2010

Published online: August 31, 2010

**Keywords:** immobilized metal ion affinity chromatography · magnetic properties · mass spectrometry · mesoporous materials · peptides

- [1] a) Y. W. Jun, Y. M. Huh, J. S. Choi, J. H. Lee, H. T. Song, S. Kim, S. Yoon, K. S. Kim, J. S. Shin, J. S. Suh, J. Cheon, *J. Am. Chem. Soc.* **2005**, 127, 5732; b) N. Kohler, G. E. Fryxell, M. Zhang, *J. Am. Chem. Soc.* **2004**, 126, 7206.
- [2] a) D. Pantarotto, J. Briand, M. Prato, A. Bianco, *Chem. Commun.* **2004**, 16; b) Z. Rosenzweig, *Nano Lett.* **2004**, 4, 409.
- [3] a) J. Dobson, *Drug Dev. Res.* **2006**, 67, 55; b) L. Zhang, S. Z. Qiao, L. Cheng, Z. F. Yan, G. Q. Lu, *Nanotechnology* **2008**, 19, 435608.
- [4] a) K. Woo, J. Hong, S. Choi, H. Lee, J. Ahn, C. S. Kim, S. W. Lee, *Chem. Mater.* **2004**, 16, 2814; b) Y. Deng, C. Deng, D. Yang, C. Wang, S. Fu, X. Zhang, *Chem. Commun.* **2005**, 5548.
- [5] a) H. W. Gu, Z. M. Yang, J. H. Gao, C. K. Chang, B. Xu, *J. Am. Chem. Soc.* **2005**, 127, 34; b) L. Zhang, S. Z. Qiao, Y. G. Jin,



- H. G. Yang, S. Budihartono, F. Stahr, Z. F. Yan, X. L. Wang, Z. P. Hao, G. Q. Lu, *Adv. Funct. Mater.* **2008**, *18*, 3203; c) L. Zhang, S. Z. Qiao, Y. G. Jin, Z. G. Chen, H. C. Gu, G. Q. Lu, *Adv. Mater.* **2008**, *20*, 805; d) Y. H. Deng, C. H. Deng, D. W. Qi, C. Liu, J. Liu, X. M. Zhang, D. Y. Zhao, *Adv. Mater.* **2009**, *21*, 1377.
- [6] a) S. Z. Qiao, C. Z. Yu, W. Xing, Q. H. Hu, H. Djojoputro, G. Q. Lu, *Chem. Mater.* **2005**, *17*, 6172; b) H. M. Chen, C. H. Deng, Y. Li, Y. Dai, P. Y. Yang, X. M. Zhang, *Adv. Mater.* **2009**, *21*, 2200; c) H. M. Chen, X. Q. Xu, N. Yao, C. H. Deng, P. Y. Yang, X. M. Zhang, *Proteomics* **2008**, *8*, 2778; d) S. Yu, G. M. Chow, *J. Mater. Chem.* **2004**, *14*, 2781; e) H. M. Chen, C. H. Deng, X. M. Zhang, *Angew. Chem.* **2010**, *122*, 617; *Angew. Chem. Int. Ed.* **2010**, *49*, 607; f) J. Wan, K. Qian, J. Zhang, F. Liu, Y. Wang, P. Y. Yang, B. H. Liu, C. Z. Yu, *Langmuir* **2010**, *26*, 7444; g) T. Rajh, L. X. Chen, K. Lukas, T. Liu, M. C. Thurnauer, D. M. Tiede, *J. Phys. Chem. B* **2002**, *106*, 10543.
- [7] a) G. P. Yao, H. Y. Zhang, C. H. Deng, H. J. Lu, X. M. Zhang, P. Y. Yang, *Rapid Commun. Mass Spectrom.* **2009**, *23*, 3493; b) J. Tang, Y. C. Liu, D. W. Qi, G. P. Yao, C. H. Deng, X. M. Zhang, *Proteomics* **2009**, *9*, 5046.
- [8] R. G. Tian, L. B. Ren, H. J. Ma, X. Li, L. H. Hu, M. L. Ye, R. A. Wu, Z. J. Tian, Z. Liu, H. F. Zou, *J. Chromatogr. A* **2009**, *1216*, 1270.
- [9] a) E. P. Diamandis, *J. Proteome Res.* **2006**, *5*, 2079; b) E. F. Petricoin, C. Belluco, R. P. Araujo, L. A. Liotta, *Nat. Rev. Cancer* **2006**, *6*, 961.
- [10] a) H. Tammen, I. Schulte, R. Hess, C. Menzel, M. Kellmann, T. Mohring, P. S. Knappe, *Proteomics* **2005**, *5*, 3414; b) K. L. Johnson, C. J. Mason, D. C. Muddiman, J. E. Eckel, *Anal. Chem.* **2004**, *76*, 5097.
- [11] X. Li, S. Y. Xu, C. S. Pan, H. J. Zhou, X. G. Jiang, Y. Zhang, M. L. Ye, H. F. Zou, *J. Sep. Sci.* **2007**, *30*, 930.
- [12] R. J. Tian, H. Zhang, M. L. Ye, X. G. Jiang, L. H. Hu, X. Li, X. H. Bao, H. F. Zou, *Angew. Chem.* **2007**, *119*, 980; *Angew. Chem. Int. Ed.* **2007**, *46*, 962.
- [13] H. M. Chen, S. S. Liu, H. L. Yang, Y. Mao, C. H. Deng, X. M. Zhang, P. Y. Yang, *Proteomics* **2010**, *10*, 930.
- [14] a) C. S. Pan, M. L. Ye, Y. G. Liu, S. Feng, X. G. Jiang, G. H. Han, J. J. Zhu, H. F. Zou, *J. Proteome Res.* **2006**, *5*, 3114; b) L. H. Hu, H. J. Zhou, Y. H. Li, S. T. Sun, L. H. Guo, M. L. Ye, X. F. Tian, J. R. Gu, S. L. Yang, H. F. Zou, *Anal. Chem.* **2009**, *81*, 94.
- [15] D. Ren, N. A. Penner, B. E. Slentz, H. Mirzaei, F. E. Regnier, *J. Proteome Res.* **2004**, *3*, 37.
- [16] M. Rainer, M. Najam-ul-Haq, R. Bakry, C. W. Huck, G. K. Bonn, *J. Proteome Res.* **2007**, *6*, 385.
- [17] K. L. Ding, B. J. Hu, G. M. An, R. T. Tao, H. Y. Zhang, Z. M. Liu, *J. Mater. Chem.* **2009**, *19*, 3725.
- [18] a) Y. H. Deng, D. W. Qi, C. H. Deng, X. M. Zhang, D. Y. Zhao, *J. Am. Chem. Soc.* **2008**, *130*, 28; b) B. Tan, S. E. Rankin, *J. Phys. Chem. B* **2004**, *108*, 20122.